Modelling flow-induced vibrations of gates in hydraulic structures

Erdbrink, C.D.

Publication date
2014

2 Background

2.1 Introduction

A prerequisite for any type of modelling is understanding the problem, which in turn requires knowledge of the system: domain knowledge. For that reason this chapter provides a background on the physical process. Because the flow forces on gates are intimately linked to the flow around the structure, the force analysis first of all builds on a study of local hydrodynamics (Section 2.2). Then, classical linear vibration theory is discussed (Section 2.3) and lastly flow-induced vibrations are introduced from the viewpoint of hydraulic gates (Section 2.4). The final section (2.5) draws conclusions from this background study of concern to subsequent chapters.

The background is inevitably concise and incomplete due to the shear scope of FIV – references are given to textbooks. The two other major sources of dynamical loads on gates of hydraulic structures, waves and ice, are left out of this study completely. These require disparate physical analyses.

2.2 Hydrodynamics: flow around a static gate

2.2.1 General description

A discharge regulating structure ordinarily consists of one or more sections (along the cross-flow direction) with uniform cross section. For gates of sufficient span, the influence of the sides (piers) as well as the presence of an adjacent gate can be neglected. Therefore it is custom to schematise a vertical-lift gate for underflow discharge by taking its cross section in the main flow direction. The area of study is hence the two-dimensional upright plane along the streamwise axis of the flow. This gives the flow model sketched in Figure 2.1, a canonical situation in free-surface hydrodynamics found abundantly in textbooks (e.g. Battjes 2001).

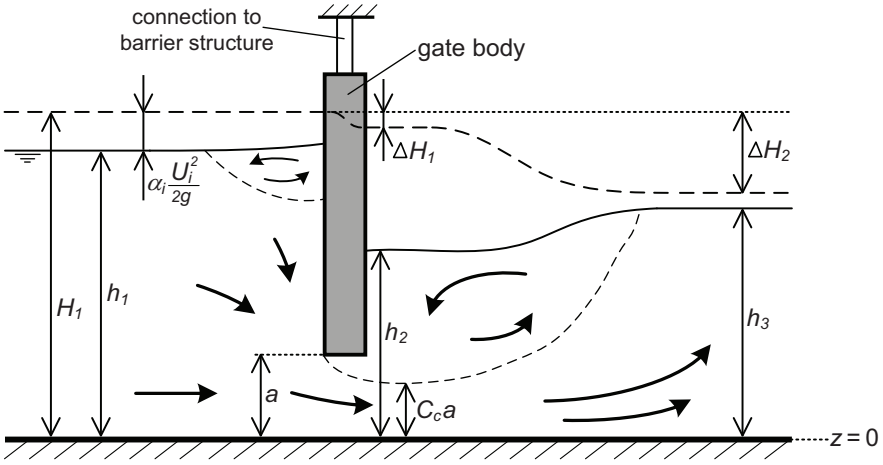

Figure 2.1. Defining schematisation of submerged flow past a vertical-lift underflow gate. The flow is from left to right.

The main flow features of the steady flow situation with a fixed gate position are shown in Figure 2.1. This figure illustrates the submerged discharge state that is characterised by sub-critical flow downstream of the gate. The designation "steady" refers to the stationary state where the flow pattern, consisting of the pressure scalar and flow velocity vector on all positions in the fluid, does not change with time. This figure will return in alternative forms, thus placing emphasis on different aspects and schematisations.

There are two drops in energy level ΔH_i, which are often lumped into one hydraulic head difference $\Delta h = h_1 - h_3$. There is a zone of recirculation downstream of the gate, characterised by a large eddy with a horizontal axis perpendicular to the main flow direction and reverse flow near the surface. The specific situation in Figure 2.1 shows submerged flow, where the recirculation exists right next to the gate, in contrast to the free flow condition where there is a detached and more violent 'recirculation' away from the gate, a hydraulic jump. The recirculation zone under submerged discharge is also called surface roller, as the fluctuations affect the free surface. The local lowering of the free surface behind the gate is due to the accelerated flow. As the velocity profile gradually returns to a fully positive profile with parallel streamlines (this is the case at h_3), the free surface also recovers. The downstream region is sometimes referred to as a 'wake', although this term is traditionally reserved for the area downstream of bodies that have flow on both sides.

There is a cross section in the separated flow layer (or emerging jet) at some distance of the gate downstream where the thickness of this layer above the floor or flow bed is minimal, this height is the vena contracta. At this point, we define $h_{\mathrm{vc}} = C_c{*}a$, where C_c is the contraction coefficient. Beyond this point, the flow diverges and decelerates. The discharge formula of flow past the gate that introduces the discharge coefficient C_d is written

$$q = C_d a\sqrt{2gh_1}. \tag{2.1}$$

Continuity or mass conservation has the general form q_i = constant = q. For the section between h_1 and the vena contracta this brings the contraction coefficient C_c into play:

$$q = h_1 U_1 = C_c a U_{\mathrm{vc}}, \text{ with } U_i = \frac{1}{h_i}\int_0^{h_i} u_i(z)dz, \tag{2.2}$$

where U_i is the depth-averaged streamwise velocity in cross section i. All basic insights on fast changing flow rely on the principle of Bernoulli, which states the conservation of energy as

$$H = h_i + \frac{u_i^2}{2g} = \text{constant, with } h_i = z_i + \frac{p_i}{\rho g}. \tag{2.3}$$

Here, H is the total head or energy head, h is the piezometric head or hydraulic head, z is the elevation above an arbitrarily chosen datum (most conveniently the bed), $p/\rho g$ is the pressure head or static pressure and $u^2/2g$ is the velocity head or dynamic pressure term. All terms were divided by $\gamma = \rho g$, the specific weight of water, so that the length unit is acquired. The subscript i here indicates an arbitrary location in the fluid. equation 2.3 in other words

says that the total energy in a point in the fluid consists of energy from the height of the fluid relative to a datum z = 0, plus energy from pressure, plus kinetic energy from the fluid's motion.

In the following, we adopt the approach by Naudascher (1991). Application of Bernoulli's principle to the section of flow acceleration between h_1 and h_{vc}, gives

$$h_1 + \alpha_1 \frac{U_1^2}{2g} = h_2 + \alpha_2 \frac{U_{vc}^2}{2g} + \Delta H_1, \tag{2.4}$$

where α_i are coefficients for the non-uniformity of the velocity distribution, U_i is again the mean velocity over the depth and ΔH_1 is the energy loss or head loss from 1 to 2 related to the forming of boundary layers along the bed and the upstream gate plate (due to downward flow) and related to the small corner eddy at the upstream surface.

In the deceleration part of the submerged flow in section 2-3, an unknown and much more significant amount of energy ΔH_2 is lost ($\Delta H_2 >> \Delta H_1$) and therefore applying Bernouli is troublesome. The momentum equation is used instead, which gives, after assuming a hydrostatic pressure distribution in the vena contracta:

$$\frac{h_2^2}{2} + \beta_1 \frac{q^2}{C_c a g} = \frac{h_3^2}{2} + \beta_2 \frac{q^2}{h_3 g}, \tag{2.5}$$

with q the discharge per unit width in $(m^3/s)/m$ or m^2/s, a the gate opening or gate height and β, like α, a uniformity measure of the velocity profile. For high Reynolds number flows, the viscous effects that give rise to $\Delta H_1 > 0$ and $\alpha, \beta < 1$ are negligible (Naudascher 1991), so that it is safe to assume ideal flow conditions for real-life situations rather than for laboratory settings, using $\Delta H_1 = 0$ and $\alpha_i = \beta_i = 0$.

The free flow version of the above goes equivalently and is simpler, since the downstream water depth after the deceleration h_3 does not influence the conditions near the gate – and hence also not the discharge. The following relation between C_d and C_c can be derived:

$$C_d = \frac{C_c}{\sqrt{1 + C_c a / h_1}}; \tag{2.6}$$

C_c is an empirical parameter from which C_d can be deduced. This approach is more respectful towards the physical causes for different discharges than simplified treatments that mention one discharge formula for submerged flow ($q = \mu a \sqrt{2g(h_1 - h_3)}$), and one for free flow ($q = \mu a \sqrt{2gh_1}$), where μ is the single empirical coefficent, usually $\mu \approx 0.6$ is taken for free flow. In more elaborate discussions, variations of the parameter C_c are investigated and explained from physical principles. Most generally, C_c is a function of a/h_1, the gate geometry and the flow bottom geometry. In the limiting case of a gate that is almost closed, $a \to 0$, the contraction is the same for free and submerged flow and $C_c = C_d$. For $0 < a/h_1 < 1$, $C_c = f(a/h_1)$ has a positive and increasing slope for submerged flow, while C_c varies much less with a/h_1 for free flow (see diagram by Rouse in Naudascher, 1991).

For free-surface flow the momentum balance can be set up for the complete stretch over which the deceleration takes place, that is, on either side of the hydraulic jump. The downstream water level past the hydraulic jump can be derived from this. In addition, the loss of energy ΔH in the hydraulic jump can be found using the Bernoulli equation. Only for special situations, depending on slope type, bed roughness and boundary conditions, analytical computations can be made of the location of the local water surface at arbitrary distances (not far) from the gate (see e.g. Chow, 1959 and Van Rijn, 2011). Usually such computations, the Bélanger equation is an example, already involve iterative schemes, so that they can hardly be called analytical.

2.2.2 Turbulence

A more realistic description is different from the fully steady case first of all because the wake circulation region always contains some time-dependent aspects: most notably vortices shed from the gate and disturbances in downstream water level. Therefore, the area downstream from the gate is sometimes said to be quasi-steady, also when the upstream conditions are steady and irrespective of the downstream flow regime.

Unsteady flow aspects are an inherent property of gate flow because of the occurrence of turbulence. Two different sources of turbulence enter the picture: free turbulence from the shear in the main flow (caused by the presence of the gate acting as an obstruction), and wall turbulence from shear due to friction along the flow bed and gate bottom. This results in the combined presence of a boundary layer adjacent to the bottom boundary of the flow (the floor) and a free shear layer under and/or directly past the gate. The extent to which a boundary layer develops along the bottom of the gate entirely depends on the surface roughness, the lay-out of the profile and the main flow velocity of the discharge. Anyway, the turbulence originating from the boundary layer and free shear layer governs the transitional zones above and under the accelerated main flow under the gate and/or directly downstream from it.

Gate profiles with a sharp edge on the upstream side, such as the rectangular gate in Figure 2.1, cause separation of the flow at that edge, the ‘leading edge’. Flow separation means that the flow no longer neatly follows the contours of a wall, but has enough momentum to leave the boundary. The pressure on this boundary is lower in the upstream part before the separation than in the downstream section after the separation. This downstream part often contains irregularities (reversed flow, possibly part of an eddy) that are not found in the main flow. Figure 2.2 gives a few examples of gate bottom profiles with the edge of the separation layer indicated. Round gate bottom profiles portray less predictable flow separation. Again depending on the precise geometry, material roughness and mean flow velocity, the flow may separate at different points along the curved gate surface. More formal: the separation point is in this case dependent on the Reynolds number. These features have been studied by various authors (e.g. Hardwick, 1974; Vrijer, 1979) to improve gate designs.

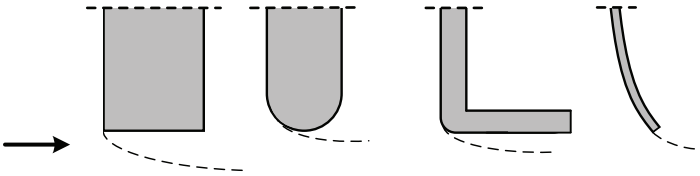

Figure 2.2. Examples of gate profiles with flow separation indicated. After design studies by Vrijer (1979).

At certain approach flow velocities and given the right geometry, the flow separation can exhibit strongly periodic detachment of rotational flow structures: vortex shedding. All construction details in the gate edge region are factors in the production of turbulence. For instance, the placement of a rigid horizontal girder on lower downstream part of the gate (meant to reduce bending of the gate) could trigger entrainment of flow from the recirculation zone into the shear layer of the submerged jet; Naudascher (1991) mentions this as a cause for a permanent low-pressure zone (under this girder) that influences the static lift force.

Calculations involving turbulence start with separating the instantaneous flow velocity in one point into a time-averaged component and a fluctuating component. This is the Reynolds decomposition, $u = \bar{u} + u'$, with $\bar{u} = 1/t^* \cdot \int u dt$ over a time length t^*. Naturally, the same decomposition is done for the other dimensions of the velocity vector. The turbulence intensity or turbulence level *I* measures, quite literally, the intensity of the fluctuations of the velocity in one point as a percentage of the mean flow. By definition,

$$I = \sqrt{\overline{(u')^2}}/\bar{u}, \tag{2.7}$$

and vice versa for the other velocity directions. The overbar denotes time-averaging again. The turbulent kinetic energy (TKE) is a scalar that represents turbulence strength of the entire velocity vector, it is defined as $k = 1/2\left(\overline{(u')^2} + \overline{(v')^2} + \overline{(w')^2}\right)$.

Omnipresent flow instabilities make turbulence a truly three-dimensional phenomenon with difficult-to-predict time-varying patterns (Tritton, 1988). There is a risk of 'analysis paralysis' (Mahajan, 2010) when trying to study all phenomena for the plethora of possible lay-outs and construction details. For example, how do the features change when the gate moves to a new position? And does it matter how fast this movement goes? Some more discussion on this follows in Section 2.5.

2.2.3 Hydrodynamic forces on a static underflow gate

Figure 2.3 shows the static forces on a rectangular vertical-lift gate. On the left, the forces are shown schematically, friction is left out. On the right, a statics diagram for the horizontal load is given.

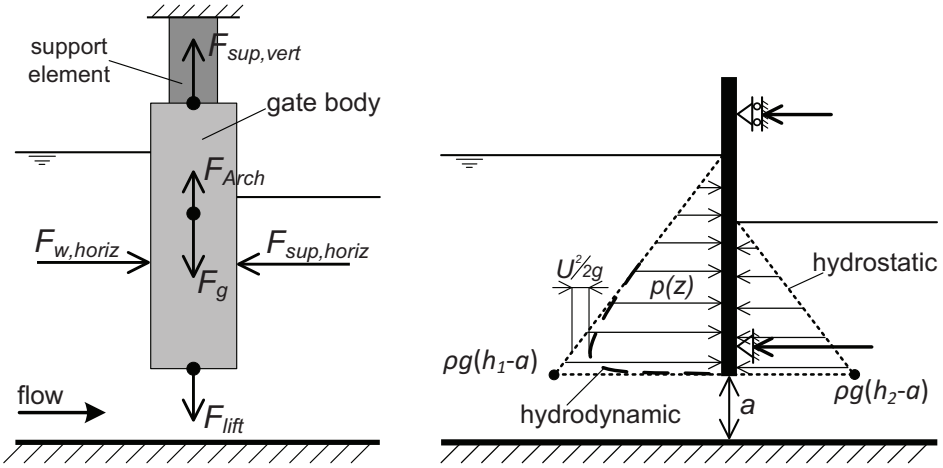

Figure 2.3. Left: Free body diagram of gate body for static force equilibrium. Right: gate as vertically placed bending beam with horizontal pressures (h_1 and h_2 as defined in Figure 2.1).

First the easier-to-estimate horizontal force on the gate are discussed by considering the total force on the upstream gate plate perpendicular to flow direction. The hydrostatic pressure distribution $p(z) = \rho g(h\text{-}z)$ gives an easily computed upper bound for the horizontal flow force. It can be used for free flow (using the upstream water level) and for submerged flow (subtracting the pressure profile of the downstream water level). This leads to a conservative estimate because the velocity head of the accelerated flow upstream has to be substracted from the integrated pressure. See Figure 2.3 (right).

The force exerted by the flowing water on the gate is found more accurately from the momentum balance between the upstream section and the vena contracta. Intuitively, the balance states that the total flow force upstream equals the force on the gate plus the total flow force at the downstream point of maximal vertical contraction. Mathematically, this looks like

$$F_{\text{sup,horiz}} = \frac{1}{2}\gamma(h_1^2 - h_2^2) - \rho q^2\left(\frac{1}{C_c a} - \frac{1}{h_1}\right) \tag{2.8}$$

for submerged flow. The free flow version of this equation follows from replacing h_2 with $C_c a$. After the horizontal hydrodynamic forces have been established, horizontal support forces are subsequently determined from the applicable structural mechanic (statics) principles. The scheme in Figure 2.3 assumes a statically determined support combination, so that two support forces can be computed in a direct manner from the force and moment equilibria.

The vertical hydrodynamic force, or lift force, requires more analysis. Following again Naudascher (1991) because of his rigorous and generic approach, the local piezometric-head coefficient C_h and its spatial average $\bar{\kappa}_B$ along the underside of the gate are introduced. The definitions are derived from converting the Bernoulli equation, applied to a section between

a point *i* at the gate bottom and the head in a point of reference downstream, into dimensionless form (after division by the velocity head):

$$C_h = \frac{h_i - h_2}{U_{\mathrm{vc}}^2/2g} \quad \text{and} \quad \bar{\kappa}_B = \frac{1}{D}\int_0^D C_h dx, \tag{2.9}$$

where D is the thickness (sometimes rather confusingly called depth) of the gate body in streamwise direction. These definitions are suitable for submerged flow, h_2 is used here as reference head. The lift coefficient $\bar{\kappa}_B$ can be positive or negative, depending on gate type, gate opening and water levels, and thus contribute to downpull (suction) or upward lift. Figure 2.4 shows the definitions for a gate with a curved underside and closed profile and is used to explain the basic computation of the lift force.

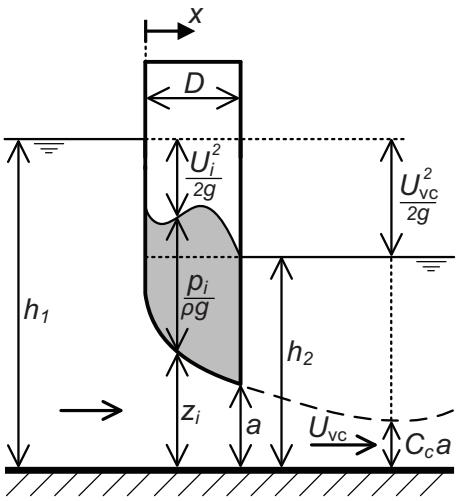

Figure 2.4. Computing the static lift force for submerged discharge, after Naudascher (1991).

The figure attempts to illustrate that the total vertical force arising from the gate being partly submerged in flowing water consists of two parts: the true lift resulting from the (non-zero) flow past the gate body and the Archimedean or buoyancy force of displacing a volume of water. For submerged flow, for the example profile in Figure 2.4, both components are upward and the total force is

$$F_{\mathrm{vert}} = \gamma B \left(\bar{\kappa}_B D \frac{U_{\mathrm{vc}}^2}{2g} + \int_0^D (h_2 - z_i) dx \right), \tag{2.10}$$

where B is the width of the gate in the horizontal direction perpendicular to the main flow (recalling that a uniform gate section was assumed). The second term is, for submerged flow, equal to the weight of the displaced water under the reference head. Now, using instead the gate opening a for reference in the case of free flow, it is found that this Archimedean term is

negative, as $a - z_i < 0$ for all i along the underside. Thus it becomes a downward force contribution.

The coefficient $\bar{\kappa}_B$ can be estimated from potential flow analysis only for non-separating flow, which is a huge limitation. So in general the coefficient, that depends on a/h_2, the gate type and the flow bottom geometry, is derived from measurements or from dedicated CFD simulations.

The separation into horizontal and vertical forces on a gate is generally not as trivial as for the rectangular, purely vertically placed gate. For the curved gate plate of a tainter gate, for instance, an extra essential point is to consider the moment of the resulting force (force relative to pivot). Moments that tend to close the gate are known to cause self-exciting vibrations when there is insufficient mass-damping (Naudascher, 1991).

A vast amount of empirical knowledge on lift forces for different gate types can be found in textbooks for many sorts of hydraulic gates and local bottom profiles (sills, aprons etc.), giving reasonable estimates of the static gate forces. When the impact of varying hydraulic conditions is considered, things become more difficult. The dynamic forces due to vibrations can be seen as an extreme case of variable conditions.

2.2.4 Navier-Stokes equations

Many books about hydraulic engineering have been written without explicit treatment or even mention of the Navier-Stokes equations. Whenever CFD is involved, however, there is no way around them. Here they are, in concise form:

$$\frac{\partial \boldsymbol{u}}{\partial t} + (\boldsymbol{u} \cdot \nabla)\boldsymbol{u} = -\frac{1}{\rho}\nabla p + \nu \nabla^2 \boldsymbol{u}\,. \tag{2.11}$$

Here $\boldsymbol{u}$ is the velocity vector in m/s, ρ is water density in kg/m^3, p is pressure in Pa, ν is the kinematic viscosity in m^2/s, ∇ is the derivative operator and $\boldsymbol{u} \cdot \nabla$ denotes the advection operator. Note that for free-surface flows of course a gravity term should be added as external force in the vertical dimension on the right hand side of (11). The fluid of interest is water, which is assumed to be fully incompressible, so that the density does not vary with pressure. The mass conservation or continuity condition is thus

$$\nabla \cdot \boldsymbol{u} = 0. \tag{2.12}$$

In chapter 4 and 6 these equations will be evaluated numerically, after substitution of the Reynolds decomposition defined in Section 2.2.2 for all velocity terms. For now, it is interesting to realise that the terms responsible for turbulence, the Reynolds stresses, are more than one hundred times larger than the viscous stresses under natural flow conditions of Re > 10^4, say (Van Rijn, 2011).

2.3 Linear vibrations

2.3.1 Basic theory

Turning now to the structural schematization, the same cross section is considered for describing the structural response. The gate body is thought to act as an isolated, rigid point mass connected to a fixed structure. The supporting connection is thought to have a certain stiffness and to provide damping. Thus the structural response is modelled as a familiar mass-damper-spring system with one degree of freedom (1 d.o.f. or single degree of freedom, SDOF), see Figure 2.5 below. What makes the situation special is that the body resonator is partly submerged in a fluid and that the fluid is (by default) in motion.

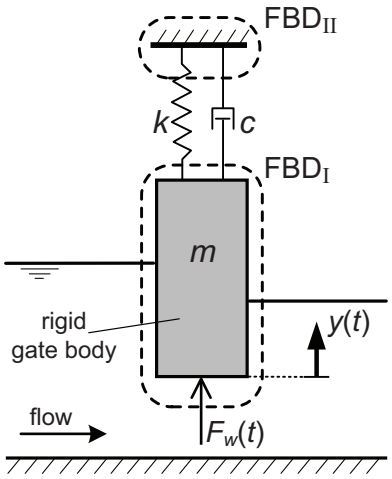

Figure 2.5. A damped mass-spring schematization of a hydraulic gate. This schematisation is consistent with Figure 2.1, only this time the emphasis is on the structural response.

This section gives a selective background on mechanical vibrations. The classic and practical textbooks by Den Hartog (1956) and Piersol and Paez (2010) are used throughout this section. Other references are given where applicable. The situation of a damped vibration with sinusoidal forcing is taken as a base case. It is assumed that the spring is linear-elastic, the damping is viscous and that the mass is concentrated in the gate (i.e. the spring and damper have no mass). In addition it is assumend the gate is in static equilibrium. This means that the gate's own weight and the stationary lift force exerted by the flowing water are balanced precisely by a static support force $F_{\mathrm{sup,st}}$ that is left out of Figure 2.5 for clarity. That is, the static deflection $\delta_{\mathrm{st}} = (mg + F_{\mathrm{lift}})/k$ is not implemented in the analytical description; the static equilibirum position simply corresponds to $y = 0$. In due course it will become clear that all these assumptions are in fact disputable.

In Figure 2.5 two free body diagrams (FBDs) are discerned. FBD$_{\mathrm{I}}$ describes the vertical force equilibrium of the gate body itself, which follows the second-order ordinary differential equation (ODE) of motion:

$$m\ddot{y} + c\dot{y} + ky = F_w(t). \tag{2.13}$$

Here, y is the vertical displacement relative to the static equilibrium position, m is the mass, c is the damping coefficient, k is the stiffness coefficient, F_w is the time-varying water excitation force equal to the boundary integral of the instantaneous pressures at the gate bottom profile. Newtonian notation is used: the overhead dots indicate derivations with respect to time. The other force equilibrium FBD_{II} in Figure 2.5 concerns the dynamic equilibrium of the support

$$c\dot{y} + ky = F_{\text{sup,dyn}}. \tag{2.14}$$

If we assume for the moment that $F_w(t) = 0$, the vibration is called free or unforced and the description of FBD_I is as follows. Introducing the natural undamped frequency $\omega_0 = \sqrt{k/m} = 2\pi f_0$, the critical damping coefficient $c_c = \sqrt{2m\omega_0}$ and the damping ratio $\zeta = c/c_c$, the solution to equation 2.13 for $0 < \zeta < 1$ (less-than-critical damping or underdamped) can be written

$$y(t) = Ce^{-ct/2m}\sin(\omega_d t + \theta) = Ce^{-\zeta\omega_0 t}\sin(\omega_d t + \theta), \tag{2.15}$$

where ω_d is the damped natural frequency given by $\omega_d = \omega_0\sqrt{1-\zeta^2}$ and C and θ are constants. The logarithmic decrement δ is defined as $\delta = \ln(y_n/y_{n+1})$, where y_n is the displacement amplitude of the n-th peak. By substitution for $n = 1$ it is found that

$$\delta = \frac{2\pi\zeta}{\sqrt{1-\zeta^2}}. \tag{2.16}$$

This implies that for small damping $\zeta \ll 1$, we have $\delta \approx 2\pi\zeta$. Returning to the forced vibration, if the external forcing is a sine $F_w = F_0\sin(\omega t)$, the motion equation 2.13 can be rewritten as

$$\ddot{y} + 2\zeta\omega_0\dot{y} + \omega_0^2 y = \frac{F_0\sin(\omega t)}{m}. \tag{2.17}$$

The amplitude of the mass motion is called the motion response and follows from the particular solution of this ODE. The general solution of (2.17) corresponds to the free vibration with solution (2.15), but in the underdamped case the natural frequency vibration dies out and only the steady-state forced vibration with angular frequency ω remains. This solution is

$$y(t) = \frac{F_0/k}{\sqrt{(1-\Omega^2)^2 + (2\zeta\Omega)^2}}\sin(\omega t - \theta),$$

$$\text{with } \theta = \tan^{-1}\left(\frac{2\zeta\Omega}{1-\Omega^2}\right) \text{ and } \Omega = \omega/\omega_0\,. \tag{2.18}$$

This result makes clear that the phase angle θ between the force and the displacement is non-zero only if there is non-zero damping. Additionally, it can be shown from (18) that in the limiting cases $\omega \ll \omega_0$ and $\omega \gg \omega_0$, $y(t)$ tends to oscillate in phase with $F_w(t)$, i.e. $\theta = 0$, whereas $\omega = \omega_0$ implies that $\theta = -\pi/2$ which means that the motion is out of phase: it precedes the force by 90 degrees. Therefore, an alternative way of writing equation 2.18 can be adopted that decomposes the formula in one sine and one cosine component:

$$\frac{y(t)}{F_0/k} = R_{\text{in}} \sin(\omega t) + R_{\text{out}} \cos(\omega t). \tag{2.19}$$

Where R is the dimensionless response factor and R_{in} and R_{out} are functions of Ω and ζ. In all above expressions the simpler equations of undamped SDOF vibrations follow trivially as a special case from $c = \zeta = 0$.

Looking now at the support force $F_{\text{sup,dyn}}$ (FBD_{II} in Figure 2.5), the magnitude of this vector is found by realising that its two components, the damping and stiffness force in equation 2.14, are out of phase by 90 degrees, which yields

$$\left|F_{\text{sup,dyn}}\right| = \sqrt{(c\dot{y})^2 + (ky)^2}. \tag{2.20}$$

It is common to define a force transmissibility quantity T as $T = F_{\text{sup,dyn}}/F_w$, from which it is possible to deduce that

$$\frac{F_{\text{sup,dyn}}}{F_0} = T \sin(\omega t - \psi),$$

$$\text{with } T = \sqrt{\frac{1+(2\zeta\Omega)^2}{(1-\Omega^2)^2+(2\zeta\Omega)^2}} \text{ and } \psi = tan^{-1}\left(\frac{2\zeta\Omega^3}{1-\Omega^2+(2\zeta\Omega)^2}\right). \tag{2.21}$$

In other words, the force transmissibility T and accompanied phase Ψ are both functions of the frequency ratio Ω and damping ratio ζ.

Figure 2.6. One of the 34 gates of the Haringvliet barrier in The Netherlands. This is a tainter valve rotating around a horizontal axis; a hinged support truss (the triangular element visible in the top of the picture) provides the movement, it is driven by a large hydraulic cylinder. Potential vibrations in the same rotation direction can be described by a SDOF system. Picture by Deltares.

2.3.2 Frequency domain

In vibration theory, sooner or later it is necessary to switch to complex notation. It makes generalisations and extensions of the analysis more compact while maintaining physical insights. Fully in line with the definitions introduced earlier we may rewrite $F_w(t) = F_0 e^{i\omega t} = F_0(\cos\omega t + i\sin\omega t)$ and assume a solution to (13) of the form $y(t) = y_0 e^{i\omega t} = y_0(\cos\omega t + i\sin\omega t)$ for the resulting displacement. The real parts of these expressions give the actual excitation and response, respectively. The imaginary part of $y(t)$ gives the phase difference between force and motion. The equivalent of equation 2.18 becomes

$$y(t) = \frac{1/k}{1 - \Omega^2 + i2\zeta\Omega} F_w(t) = X(\omega)F_w(t), \tag{2.22}$$

where now in the last step the mechanical admittance X is defined, a function with the frequency as independent variable. Notation from Naudascher and Rockwell (1994) is largely followed. From the insight that the absolute value of $X(\omega)$ is the ratio of the amplitudes y_0/F_0, which is the quotient term hidden in equation 2.18, it follows that

$$X(\omega) = |X(\omega)|e^{-i\theta}, \tag{2.23}$$

with θ according to equation 2.18 and $|X(\omega)|$ is called the complex frequency response or receptance. Substitution in equation2.22 then gives the desired solution

$$y(t) = |X(\omega)|F_0 e^{i(\omega t-\theta)}. \quad (2.24)$$

An obvious trick is to use Fourier analysis to make the extension to arbitrary periodic forcing functions. The first step is to decompose $F_w(t)$ by writing it as a Fourier series. As long as the motion equation is linear (that is we assume a linear time-invariant or LTI system), the total response is equal to the sum of the responses of individual harmonics (multiples of a base frequency). This always gives a periodic response $y(t)$. A further extension is to consider non-periodic excitation functions. Here the Fourier integral can be used for decomposition of the force signal as a function of the frequency. Switching now to the frequency f = ω/2π, more common for spectra, the spectral densities S of the excitation F_w and the response y obey the equation

$$S_y(f) = S_{F_w}(f) \cdot |X(f)|^2 \quad (2.25)$$

The power spectral densities have the useful property that the integral over the entire spectrum equals the squared value of the root-mean-square value of the signal.

2.4 Physics of flow-induced gate vibrations

2.4.1 Introduction to flow-induced vibrations

Fluid-structure interaction (FSI) is a wide and active field of research with a huge number of applications. It can be interpreted as an umbrella term for physical systems where the mutual dynamics of fluids and solids plays a central role. In computational contexts, FSI is often reserved for problems where the structure has a certain flexibility to deform, such that the changes of the fluid-solid interface in time and space are the main interest. It is important to be aware of the fact that different properties of fluids (viscosity, density) and solids (stress-strain, d.o.f.s) make for drastically different FSI problems. A numerical model of a flapping airplane wing may be fully calibrated and have high accuracy; it will in many respects be useless as a basis for a model of a pontoon floating in water. Examples of FSI problems that illustrate these ranges are the bending of slender structures in flow (e.g. airplane wings), bloodstreams inside the body, and wind-induced motion of high-rise buildings. Païdoussis et al. (2011) give a general treatment of FSI.

The field of flow-induced vibrations (FIV) focuses on the motion of objects in flow with limited degrees of freedom. The solid is an object that is too stiff to have the flow cause wave-like phenomena on the fluid-solid interface. Rather, the object undergoes a translational, rotational, or bending motion or a combination of these three. This is why the presented mass-spring model is a salient fundament for FIV problems. Authorative textbooks on FIV are Blevins (1990) and Naudascher and Rockwell (1994). The classical case study object in FIV is a cylinder, defined as a solid object with one of its three dimensions uniform and elongated, and which can have all sorts of cross-sectional shapes, the most familiar being a circle and a square. All objects with considerable blocking of the flow –characterised by flow separation for flow from all angles– are named bluff bodies, in contrast to aerofoils which have a streamlined wing-type shape.

Experiences from practice with real-life prototype data and evaluation of FIV causes form an invaluable category of FIV studies. As part of many investigations into dynamics of hydraulic structures in The Netherlands built in the second half of the 20th century, Kolkman and Jongeling (1996) give a sizeable account of FIV with ample attention for gates. More recently, Kaneko et al. (2008) compiled engineering experiences of FIV from Japan. Because there was and is often a strong consciousness only for preventing vibrations from growing beyond safety limits, in-depth physical analyses and development of general computational methods have not received too much attention.

Vortex-induced vibrations (VIV) deal with those flow-induced vibrations of (cylindrical) bluff bodies with flow on both sides. The canonical case in hydrodynamics of the Von Karman vortex street of flow around a circular cylinder can be extended by giving the cylinder freedom to move in cross-flow direction; as such it has become canonical in VIV too. Academic research in this area has been driven enormously by industrial applications in nuclear power plants (cylindrical heat exchangers) and in offshore engineering (e.g. pipelines, marine risers). Moreover, the two canonical cases mentioned are frequently used as benchmarks for computational models owing to the complexity of the physics and the availability of measurement data. A frequently cited overview of analytical and to some extent also numerical models of VIV is given by Sarpkaya (2004). Gate vibrations are a distinct subset of FIV with little overlap with the VIV subset. Gates are essentially different because the flow exists only on one side of the object and there is a significant influence by the presence of at least one wall.

The remainder of Section 2.4 uses and combines knowledge found in Blevins (1990), Naudascher and Rockwell (1990) and Kolkman and Jongeling (1996).

2.4.2 Dimensionless parameters

A good way to start is by identifying the most relevant dimensionless parameters. Table 2.1 lists these alphabetically.

Table 2.1. Dimensionless parameters of gate vibrations.

	symbol	definition
dimensionless amplitude	-	A/D
damping ratio	ζ	$c/2\sqrt{km}$
Froude number	Fr	$U/\sqrt{gh}$
mass ratio	m_r	$m/\rho D^2$
reduced flow velocity	V_r	U/fD
Reynold's number	Re	UD/ν
Scruton number	Sc	$4\pi m_r \zeta$
Strouhal number	St	fD/U
turbulence intensity	I	$\sigma_u/\bar{u}$

In the table, gate thickness D is used as characteristic length scale, except for Fr where the water depth h is used. The standard deviation of u, denoted σ_u, is used in the turbulence intensity formula. The difference between V_r and St is important. Both are dimensionless velocities or, alternatively, dimensionless frequencies. The reduced flow velocity V_r deals with response: it uses the response frequency and $U = \sqrt{2g\Delta h}$ as characteristic velocity, whereas the Strouhal number deals with excitation: it uses the excitation frequency and the steady undisturbed upstream velocity as characteristic velocity U. The Strouhal number is linked with periodic excitation or forcing from vortex shedding. Its numerator can be interpreted as the speed at which disturbances from separation at the upstream edge move along the bottom gate boundary. The reduced flow velocity indicates the velocity of flow under the gate relative to the gate motion, similarly it is a dimensionless measure of the frequency of the gate motion.

The mass ratio and the damping ratio are decisive for the actual response that is realised. The mass ratio gives the mass per width unit relative to the surrounding fluid and is an inertial measure of how easily the gate body initiates into motion. The Scruton number combines mass and damping ratios. It is popularly used in VIV, but has the disadvantage that the effects of mass and damping are no longer distinguishable. Specifically for gates, damping is of so much importance that one would like to quantify it separately. The Froude number describes the influence of the free surface, not in all cases directly impacting the vibrations, but nevertheless relevant for free flow and intermediate conditions.

The infamous Reynolds number is in this context mainly relevant in physical models for ensuring that viscous effects are relatively small. Of course in physics-based numerical modelling, the success of any approach (other than direct numerical simulation, DNS) that attempts to estimate the Reynolds stresses depends strongly on *Re*. The higher *Re*, the broader the range of length and time scales in the flow.

The most concise way to summarise all FIV efforts is to state, as an adaptation to Blevins (1990), that we aim to find the amplitude as a function of the other parameters:

$$\frac{A}{D} = f(\zeta, m_r, V_r, \mathrm{Fr}, \mathrm{Re}, \mathrm{St}, I), \tag{2.26}$$

where the Scruton number is left out because it is a function of the mass ratio and the damping ratio. From a reverse point of view, we are just as well interested in determining the function *f*, given values of the dimensionless parameters.

In addition to providing general physical insight, the dimensionless parameters have a strong importance in the design, interpretation and comparisons of physical models in the laboratory. When scaled-down models (physical and numerical) are compared to prototype structures, the dimensionless parameters are ideally scaled by equal factors –something which is quite impossible in most circumstances– in order to keep scale effects to a minimum. In particular, for dynamics of structures, scaling of elasticity and damping requires meticulous efforts.

2.4.3 Causes of flow-induced gate vibrations

Various categorizations of FIV are presented in literature. The emphasis in the most useful categorizations is on the causes of vibrations, which are described in detail in excitation mechanism theories. A complicating factor when browsing through literature is that many past analyses were done based on unjustified assumptions regarding excitations. Also, the terminology regarding vibration causes is not undisputably agreed upon. Here, the excitation categories are introduced by Figure 2.7.

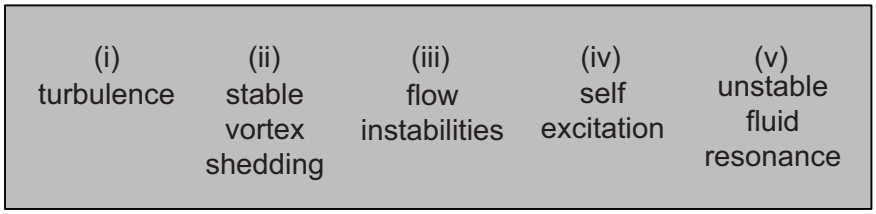

Figure 2.7. Causes of flow-induced vibrations of hydraulic structure gates.

The proposed subdivision in Figure 2.7 is close to that by Kolkman and Jongeling (1996), with the only addition that (i) and (ii) are treated separately. Points of discussion leading to other subdivisions have to do with how turbulence and flow instabilities are defined. In literature, mechanisms are sometimes attributed to the classes movement-induced excitation (MIE), instability induced excitation (IIE) and impinging leading edge vibrations (ILEV) introduced by Naudascher (see Naudascher and Rockwell, 1994). Although these have their value as shorthands for some the causes discussed here, and they will be used in Chapter 5 and 6, they are together not all-inclusive for all encountered phenomena. Excitations (i)–(v) are briefly discussed only up to necessary detail for further work; in-depth discourses are found in the textbooks already mentioned.

(i). Excitation by turbulence

Hydraulic gates are constantly in contact with flowing water. This fact alone is a source of excitation because the incoming flow is in reality never free of fluctuations around the mean value (see equation 2.7); $I \approx 10\%$ is already considered high-level turbulence). In an ideal Reynolds decomposition, all periodicity is filtered out, such that $u'(t)$ is a noisy, random signal with a uniform frequency distribution. The dynamic force on the gate associated with this excitation is said to be caused by external turbulence excitation, assuming that the source of the turbulence lies outside of the structure, that is, the non-periodic fluctuations were already present in the flow before reaching the structure. Computationally, equation 2.25 in Section 2.3 for random signal excitation is applied:

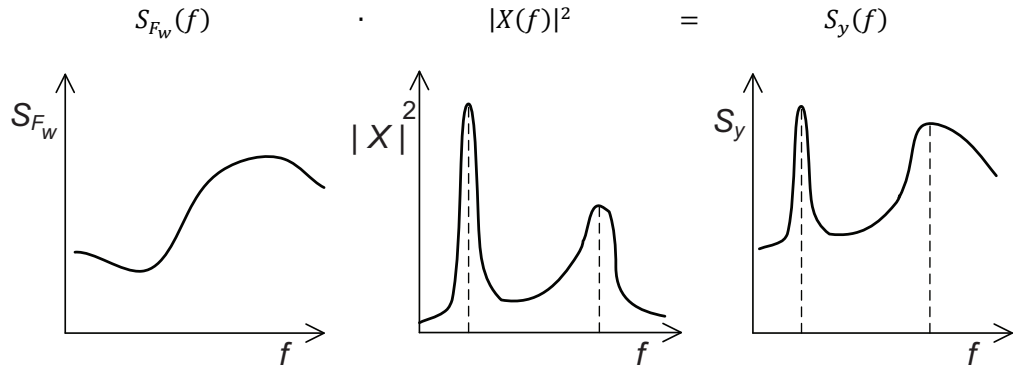

Figure 2.8. Illustration of a response spectrum derived from a spectrum excitation for a (gate structure) system with two eigenfrequencies.

Figure 2.8 gives a devised example of computations in the frequency domain. When the natural frequencies of the system *X* (determined by the gate and its suspension structure) are known, the response spectrum S_y is found through multiplication with the force spectrum $S_{F,w}$. The particular illustrative example of Figure 2.8 shows that the response to a broad-band excitation reveals the natural frequencies of the structure in the output signal.
The occurrence of low-level, irregular loading on a hydraulic gate is an everyday phenomenon, hardly noticeable and not harmful to the structure. This is a passive interaction: the responses (displacements, deformations, stresses and support forces) have no influence on the dynamic loading. Excitation by this random-type turbulence leads to dynamic forces of just a few percent of the stationary lift force, Kolkman and Jongeling (1996) mention a maximum of 10%.

(ii). Excitation by stable vortex shedding
The mere presence of the gate is an interference of the incoming flow by a bluff body, creating disturbances of a periodic nature in the form of vortices and eddies, see Tritton (1988). If the sizes of these periodic parts of the flow ('coherent structures') are unambiguously related to the size of the object from which they are shed (a characteristic length scale of the gate, commonly its thickness D), and their propagation speed is proportional to the mean incoming flow velocity U, then the Strouhal number is a constant and hence useable for describing the excitation frequency. Key to this condition is the shape on the upstream gate side that is decisive for the type of flow separation. As depicted in Figure 2.2, a sharp leading edge fixes the point of separation, resulting in stable vortex shedding, whereas round elements make the separation point dependent on Re (even at high Re when viscosity is no factor), resulting in unstable vortex shedding, treated under (iii).

Elaborating on the stable type of vortex shedding, a thick enough gate bottom will feel the periodic impact of the separated layer as it periodically bends back to the gate's underside at small gate openings. This is called impingement (ILEV). The periodic excitation force is in this case found from *St*. There are flow measurement data giving

$$\mathrm{St} = f(\mathrm{a/D}, \text{geometry})$$

for a number of gate types that give stable separation. To grow some intuition, consider a gate at a small opening, say $a/D = 0.4$, with initially zero head difference Δh. As the upstream water level slowly increases, Δh and U will increase, and –according to the constant St– so will the vortex shedding and excitation frequency f_{exc} (= $\omega/2\pi$ in Section 2.3). The critical question is now whether U can grow so high that f_{exc} approaches f_0. This will ultimately lead to resonance amplitudes dictated by the damping in the system. To stay away from this situation, the stiffness of the construction elements is preferably high enough to have at least $f_0 > 2f_{exc,max}$, where $f_{exc,max}$ corresponds to the maximum flow velocity U. This kind of analytical model is called a vortex-shedding model by Tondl et al. (2000), they use it as a base for various vibration analyses.

Given the knowledge on St-values and above design instruction, significant vibrations due to this excitation can be avoided. Note that the relation between flow field and gate geometry is not always 'neat', there could be a band of excitation frequencies rather than a single f_{exc} for a given approach velocity U. This is no surprise because the shedding of vortices is principally a turbulent effect arising from flow past the structure (a kind of 'internal turbulent excitation' as it were, although this term is never used). The Strouhal number can in this case still be applied to the dominant frequency of this band, however. In conclusion, turbulence-related forcing by excitations (i) and (ii) is unlikely to cause vibration-related trouble, as long as the structural eigenfrequencies indeed lie outside the spectral band of these excitation frequencies.

(iii). Excitation by flow instability
For underflow gates, three flow instability cases are relevant:

- The separation point does not have a fixed position if it depends on the inflow conditions (Re), this is the case for a rounded leading corner (Figure 2.2). This gives rise to an instability of the separated flow as a whole. The pressure difference on the gate inherent to the flow separation is now time-dependent. This is itself already a periodic forcing.
- The separated flow after some distance slowly starts losing its momentum due to exchanges with the surrounding flow (by formation of tiny eddies), and widens as it decelerates. If this all happens under the gate, and the upward bending causes reattachment of the shear layer to some part of the gate construction, than this too can lead to instability if this reattachment is not fixed in space somehow.
- A third cause of instability takes place when the reattachment is fixed to one position by a protruding element (e.g. lip at trailing edge). The region between separation point and reattachment point forms a closed volume of rotating flow with the moving gate bottom on one side and the shear layer feeding energy into this region on the other side. The enclosed area develops periodic pressure fluctuations which exhibit distinct, i.e. discrete excitation frequencies connected to how many wavelengths of the pressure waves are active in the given space.

A distinguishable feature compared to (ii) is that a motion of the gate can have influence on the cycles of these flow instabilities and therefore on the resulting periodic forcing: active interaction. In particular, the excitation frequency can adjust itself to get closer to the motion

frequency, the 'lock-in'. In order to analyse these flow instabilities with CFD, the turbulence-related features that define the separation and the shear layer must be well represented.

(iv). Self-excitation
Self-excited or self-induced vibrations are widely studied because they describe many problems in engineering and physics. They are also interesting objects of study in their own right, in dynamical systems analysis (Verhulst, 1996). This vibration type is defined by the driving force originating from the displacement of the oscillating body itself (Den Hartog, 1956). That is, a self-sustained system exists without the need for external forcing. New energy is fed into the system by an energy transfer from the water flow to the gate motion, which is most easily described in the linear ODE of motion (equation 2.13) by a negative damping term. This is clearly an active interaction that could lead to exponentially increasing amplitudes. The general rule is that all forms of self-excitation of gates are potentially dangerous and should always be avoided.

Three theories of self-excitation are discerned for gates.

Galloping
Eminated from a study of vibrations of telephone wires covered in ice, Den Hartog (1956) explained that the observed low-frequency oscillations could not be caused by vortex shedding. Instead, galloping is a dynamic instability, linked closely with the object's lay-out, where the varying orientation of the incoming flow relative to the moving body gives an amplifying lift force in the same direction as this movement. The condition for which dynamic instability occurs, as derived by Den Hartog (1956) reads

$$\frac{\partial C_L}{\partial \alpha} + C_D < 0. \tag{2.27}$$

That is, the change in the lift force coefficient C_L as a function of the angle α between the apparent or relative velocity U_{rel} of the approach flow relative to the body's velocity is no longer balanced by the drag force component C_D. For a rectangular gate profile of a vertical-lift gate, an up and down movement may cause cyclic variation in the suction (lift) force: in the downward swing the region between gate bottom boundary and shear layer narrows, local pressure decreases and downward suction increases and vice versa for the upward motion. To the extent that the time lag between excess lift and motion gives rise to a net force proportional to object velocity, there will be negative damping and self-excitation.

Fluctuating leakage gap
The dynamic forces on a plug valve (or stopper) when emptying a bathtub are described by Kolkman and Vrijer (1977). A spring-mounted gate or valve initially covering the upstream side of a culvert regulates the discharge from the upstream reservoir to the culvert. The inertia of the flowing mass of fluid past the gate causes a lift force on the gate proportional to the velocity at which the gate is raised – at a small distance from the opening to the culvert. Setting up ODEs for the discharge variation, the flow in the culvert and the position of the gate results in a third order ODE with physical coefficients and a stability criterion for the spring stiffness.

A generalisation step is needed to extend this theory from a gate closing off pipes and culverts on the upstream side, to vertical-lift gates in free surface flows. The in-line inertia is now thought to be caused by a fluid volume in a fictitious streamwise tube of length $D + (C_{Lu} + C_{Ld})a$, where the C_i are length coefficients.
Figure 2.9 gives an impression of the effect. Under the assumption that the local head difference at the gate consists of a constant global head difference plus a dynamic term caused by the dynamics of flow acceleration and deceleration related to discharge variations $\mathrm{d}q/\mathrm{d}t \sim \mathrm{d}a/\mathrm{d}t \sim \dot{y}$, it is found that there has to be an oscillatory term in the suction (lift) force that enables the changes of momentum of the imaginary tube. A lumped suction force coefficient was computed as a function of a Strouhal-type dimensionless number related to the gate opening and compared to experimental values. This theory is also discussed in Kolkman and Jongeling (1996), but has had little following, despite the appealing intuition at the heart of it.

Fluctuating discharge coefficient
Another way of thinking about how the movement of the gate cuts off the discharge is through an oscillation of the discharge coefficient. This is for instance found in in-flow vibrations of underflow gates with rounded bottom profiles. A moving point of flow separation then causes a varying contraction and so a varying discharge coefficient, leading to pressure fluctuations across the gate in phase with the vibration velocity. The working of this mechanism and the previous one depends on the frequency of the motion: when this becomes too high, the inertia or discharge capacity effects have no time to initiate.

The last two theories are quite complicating effects specific to gates. They have by far not been studied as much as for instance galloping and vortex shedding. All three theories in (iv) have in common that the internal driving force depends on the motion amplitude. That is, compared to the simple free motion of equation 2.13 with $F_w = 0$ there exists an extra force $F(y)$ proportional to y or $\dot{y}$, which often implies non-linearity.

(v). Unstable fluid resonance
Global instabilities of the fluid in which the gate is located can give rise to gate vibration with a frequency dictated by the natural frequency of the fluid reservoir. Examples are seiches, standing waves of the free surface, standing compression waves. Incorporating this mechanism in the evaluation of gate stability requires a broader view on the hydrodynamics than for the other mechanisms, where analysis of detailed local flow was needed.
Initially small gate vibrations may also be amplified rather than initiated by fluid oscillations ('self-control') in the reservoir adjacent to the structure. If the characteristic frequencies of gate and fluid resonance coincide, mutual energy exchange contributes to further amplitude growth. This phenomenon has been recognised relatively recently. Jongeling and Kolkman (1996) provide studies of real-life cases.

2.4.4 Added coefficients
The presence of the body in water gives added coefficients that, indeed, have to be added to the basic coefficients of the linear ODE of equation 2.13. The added coefficients m_w, k_w and c_w are key to quantifying and understanding vibration (causes) of bodies submerged in water. They influence the natural frequency, the restoring forces and govern energy exchange with

the flow. Kolkman (1976) established insightful connections between the added coefficients and the dimensionless parameters in Table 2.1.

Following the compact overview by Kolkman in Novak (1984), they are merely introduced here to prevent repetition of already existing, apt treatments.

Added mass m_w
When a body is moving through a fluid, it has to push some portion of the fluid out of its way. The mass of the fluid volume pushed away by the body (during oscillation) is called the added mass, written m_w. This inertial effect causes the natural frequency of a vibrating object in water to be lower than in air. In Figure 2.9 the three inertial effects identified for a cross-flow gate vibration are illustrated.
There is no straightforward analytical way of quantifying the added mass in general. Only for very basic object shapes in a stagnant fluid, analytical formulas exist for m_w, under certain assumptions. An oscillating strip of length L and width D, for example, is thought to mobilise a semi-cylinder of fluid, thus yielding $m_w = (\pi/4)\,\rho D^2 L$. Both potential flow theory and FEM have been used to estimate m_w for numerous applications. The value of m_w is in any case affected by confinements of the surrounding fluid domain: the floor and walls. Consequently, m_w can depend on gate position y, thus introducing a non-linearity. Other factors that may or may not come into play are wave radiation (the production of small amplitude free-surface waves by the vibrating body) and, related to this, dependency of m_w on vibration frequency.

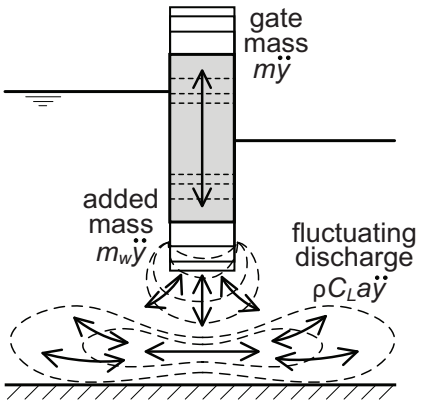

Figure 2.9. Three inertial effects connected to accelerations of solid and fluid.

Hydrodynamic rigidity k_w
Also called added stiffness or hydraulic stiffness, three instances of k_w are encountered.

- A floating body that is pushed downward into the water experiences a higher upward Archimedean force. Combining Archimedes with Hooke's law, it is derived that a downward displacement Δy of a semi-submerged body gives an extra upward force equal to $\rho g A_w \Delta y = k_w \Delta y$, where A_w is the horizontal wet cross section of the object. It follows that k_w does not depend on gate position y and is proportional to the area A_w cutting the water surface.
- A spring force is a restoring force; a wind vane rotating in the wind experiences a positive added stiffness force pushing it back to the stable equilibrium position parallel

to the ambient wind direction. When a lift force on a (wing) profile increases proportional to the rotation with respect to the mean flow direction, it will give the same effect.

- At high gate frequency there is a third k_w effect called instantaneous rigidity connected to the theory of the fluctuating leakage gap. Suppose a culvert between two basins with a head difference is partly closed off by an in-flow gate on the downstream side of the culvert. A sudden change of the gate position Δx that makes the gap smaller results in a sudden pressure increase Δp (due to the same discharge going through a smaller gap), assuming the discharge fails to adapt to the new gate position immediately. The extra pressure acting on the gate surface A_{gate} gives a force in phase with the sudden displacement Δx and in working in opposite direction. Thus, this is a restoring force with added rigidity $k_w = \Delta p \cdot A_{\text{gate}}/\Delta x$. An equivalent analysis for an upstream culvert gate shows that in this case the rigidity k_w is negative.

Added damping c_w

Positive-valued contributions to hydrodynamic damping c_w are radiation of kinetic energy from the gate as free-surface waves (wave radiation), skin friction and damping by drag. In the last case it is necessary to take the projection of the drag force in the flow direction, say F_y, and apply $c_w = -F_y/\dot{y}$. This is a turbulent hydrodynamic damping proportional to the square of the velocity. Negative values of c_w are inextricably linked to self-excitation. How c_w is computed is different for each of the three self-excitation mechanisms. In the end, it comes down to checked whether $c + c_w < 0$ can occur, where c is the structural damping in the mechanical system of gate and suspension. This would lead to a dynamic instability with increasing amplitudes. Analogously, $k + k_w < 0$, with k the structural rigidity, would give a static instability. The term structural damping is also used for an analytical model known as hysteresis damping, the damping force then depends on displacement instead of velocity (e.g. Adhikari 2000, Rijlaarsdam 2005). This meaning is not used in this thesis. It is wise to leave all options open regarding damping models; to name one more: Coulomb or dry damping is described by $F_{\text{damp}} \sim \text{sign}(\dot{y})$. Sometimes energy considerations come in hand. The work done by the damping force on the body during one cycle is equal to

$$\int_0^T F_{\text{damp}}(y, \dot{y}, t) \cdot \dot{y}(t) dt \tag{2.28}$$

over a motion period T. This can quantify a dissipation of energy or a transfer of energy to the motion $y(t)$.

It is noted that added mass and damping can cause pressures on the gate in a different direction than the vibration direction. The notorious example is the added mass of a vertically vibrating L-shaped object. This is a basic example of a coupling effect; the forces due to the added mass in still water now require a 3x3 coefficient matrix relating horizontal and vertical forces and an in-plane moment to x and y-translation and rotation.

2.4.5 Consequences of gate vibrations

Small irregular background vibrations, as described by (i) in 2.4.3, are impossible to avoid and are not harmful. Other FIVs may also have innocent consequences, but the problem is that we cannot arrive at this conclusion without knowing the exact forcing characteristics,

assessing them in structural analyses, and comparing computed stresses with design values. Distinguishing three failure categories, to which of course a rest category of unknown failure modes has to be added, FIVs of gates will be called unsafe when one of the following scenarios comes into effect.

- A (part of) the gate or adjacent structural elements is excited into a vibration with amplitudes exponentially increasing over time, until the point where this growth stabilizes due to extra internal or external mechanical damping. At that moment, the sheer momentum and kinetic energy of the oscillation can be enormous. This is typical for vibrations of the self-excited type and should always be avoided. It is probable that the structural elements involved in this process (including hinges, pivots and supports) were not designed to withstand this. Particular for this type of loading is the periodic load change; combined with a long duration there is a danger for fatigue (according to Kolkman and Jongeling, 1996). Failure of one element may set off a malicious chain of events leading to failure of other elements. In an extreme case reported by Ishii et al. (1980), a main truss fails under buckling and the gate body as a whole disconnects from the structure and is washed away downstream.
- Gate vibrations hold up or hinder operation. As a result of vibrations, a gate can get stuck in one position or partly break itself by smashing into the sill. It then ceases to function as a discharge controller. If no timely action is taken, such as installation of an emergency gate, the discharge can become uncontrollable during a significant amount of time. Apart from secondary inconveniences (e.g. shipping traffic), the immediate danger is that local flows exceed design limits of the bed protection. This is a serious threat to the stability of the overall structure.
- Another type of 'failure' comprises the psychological impact of unexpected vibrations. Hydraulic structures are seen as incomprehensibly strong and rigid structures that were built to protect land and citizens. Any observation of vibrations, for instance by whistling noises or small waves at the water surface, may lead to concern from the managers of the structure – with or without good reason.

2.4.6 Myths about gate vibrations

The fact that linear vibration theory and flow around a gate are taught in elementary rather than advanced courses in respectively mechanical and civil engineering might mistakingly lead to the idea that gate vibration is not a complicated subject. Much on the contrary, it is a deceptively complex topic. Five popular misconceptions are given.

(1). Addition of damping can solve any vibration issue of hydraulic gates.
Adding damping is foremostly a (trivial) theoretical measure that, for large hydraulic structures, is rarely a feasible and acceptable solution; not only because a suitable damper would have to have huge proportions, but also because it would inhibit normal opening and closing movements.

(2). If gates vibrate, they vibrate at their natural frequency.
This is false as a general statement, for a number of reasons. First of all, 'natural frequency' usually refers to the undamped natural frequency in air. The natural frequency in water is different due to m_w and k_w. Secondly, the gate can be excited by fluid resonance, in which case the gate frequency adopts the resonance frequency of the fluid basin.

(3). Problems with FIV in hydraulic structures are caused by turbulence.
This is false. In practice, gates or other components of hydraulic structures are seldom excited into problematic vibrations by turbulence alone. Non-periodic noisy turbulent fluctuations in the approach flow are as it were overpowered by local flow acceleration at the gate and thus act as a relatively small external load. Vortices by themselves give a passive forcing that does not grow to troublesome proportions.

(4). Intelligent gate operation can always avoid vibrations.
Of course it is wise not to choose critical (that is, often small) gate openings for long discharge scenarios. As a first solution approach it is therefore good to see if dynamic loads can be avoided or reduced by smart operation. This is investigated in Chapter 4 and 7. However, some excitation scenarios are not easily avoided or recognised on time.

(5). A designer that knows the dangers of vibration-sensitive gate profiles can easily prevent undesired dynamics.
To some extent this is true; the probability of FIV is greatly reduced by a good gate design, preferably tested in a physical model. But the combined effect of realised structural details and local flow conditions can still cause phenomena that are hard to predict and evaluate before construction. Consequently, vibration risks can never be ruled out completely. Moreover, there are several stringent constraints that usually claim more attention in the design process than FIV loads.

2.5 Generalisation and problem solving in practice

The single mass-spring schematisation was chosen because it can suitably represent most fluid-structure interaction mechanisms for gates. More complex and realistic schematisations can be constructed by adding multiple SDOF systems together, as is commonplace in structural mechanics. The specific choice for a vertically moving gate object is on the one hand motivated by the fact that vertical-lift gates with underflow constitute a large class of gates, and on the other hand by the fact that this configuration gives the most straightforward and generalisable description that can be adapted for application in the vibration analyses of other gate types. This might seem strange. For estimating discharges and hydrodynamic forces other than those caused by waves, ice and vibrations, different gate types have to be treated separately. Indeed, textbooks such as Naudascher (1991) enumerate gates of many shapes and sizes and contain various, *different* formulae for estimating the forces on the gate and the support forces. However, for FIV analysis there is often little sense in repeating the analytical discussions of Sections 2.4.3 and 2.4.4 for other gate types, for instance for a rotating tainter valve (see Figure 2.6), because there is significant overlap in the conditions under which vibrations arise and therefore principally the same excitation mechanisms (Figure 2.7) are distinguished for different gate types. In other words, the single mass oscillator submerged in a flow is a fairly universal representation. Sometimes one encounters SDOF schematisations for theoretical analysis based on a gate type other than the vertical-lift gate, however; for example Kolkman (1976) in one of his appendices studies a reversed tainter valve in a culvert. Despite a different (less trivial) equilibrium of static forces, the vibration mechanisms of this gate are similar to that of the vertical gate. More complex cases involve continuous or distributed masses (see

Naudascher and Rockwell, 1994), among which are plates, beams and shells. Because of the presence of water, theoretical dynamic response analyses of such elements quickly become impractically hard.

The main limitation of the vertically suspended gate schematisation is that it only considers cross-flow vibrations. In-flow vibrations, in Figure 2.1 these would be horizontal, have been and are treated separately in academic literature (e.g. Jongeling, 1988). A small number of excitation mechanisms (not part of this thesis) is thought to exist exclusively for in-flow vibrations, but it cannot be denied that in-flow and cross-flow vibrations share many features. When a gate body experiences both degrees of freedom (cross-flow and in-flow) simultaneously, the situation is fundamentally more complicated. Acceleration in one direction may ignite acceleration in the other due to coupling effects stemming from the added masses. It is mentioned by Kolkman and Jongeling (1996), with reference to a study of Ishii and Knisely (1992), that a ratio of eigenfrequencies of both directions close to one has to be avoided.

The analytical metaphor of the gate as a spring-mounted discrete body forms the starting point of practical FIV studies of all kinds of gate types. The engineering practice basically requires a combination of this foundation and ad hoc detective work. Of course knowledge about how different gate types work and what hydrostatic forces they experience is also needed. But from theory it is impossible to link one gate type to one vibration mechanism; everything that was treated in Sections 2.3 and 2.4.1-2.4.5 is potentially applicable to all gate types.

A few examples of typical recurring phenomena encountered in practice:
- discharge variations due to local leakage between gate and sill,
- periodic pinching of slits (between gate and side support or between two adjacent gates),
- lack of aeration on the downstream side of gates with overflow discharge; this can give periodic variations of the enclosed air volume, leading to pressure variations on the gate.

In case of suspicion of gate vibrations, the curing procedure needs to at least look at questions like
- What are the least stiff bending directions?
- Where is room for movement (sideways, rotational, etc.)?
- Are there pivots that allow a certain extra freedom of movement?
- Is there an asymmetry of (leakage) flows?
- Do the shape and material of the sealings allow flow instabilities or unwanted discharge variations?

This results in an overview of the most likely eigenmodes. Apart from possible oscillations of the gate as a whole, it is necessary to scrutinise the elastic properties of all structural elements (especially those with relatively low stiffness) that come in contact with the main flow, e.g. plates near gate edges, supporting trusses, etc. Additionally, for each potential vibration element, it has to be checked which of the mechanisms may lead to excitation. All these issues are commented on and illustrated by case studies in Kolkman and Jongeling

(1996). The same authors note that if a field study results in a correct diagnosis of vibration sources, the implementation of a countermeasure is often simple and inexpensive.

Experience clearly plays a large role, and proper judgements require the ability to distinguish major issues from secondary issues, but this is no substitute for sound reasoning and computation based on the rather wide theoretical background sketched in this chapter. In their concluding remarks, Naudascher and Rockwell (1994) advocate the proper use of the excitation theories: "Had FIVs been discussed exclusively in terms of affected systems and structures, the reader would have been misled into thinking that by eliminating the various *specific* causes for excitation, it would be possible to safeguard similar systems against vibration problems. We wish to reemphasize that in order to come close to the goal of ascertaining *all possible* origins of FIVs, one must, first, thoroughly identify all the various body oscillators and fluid oscillators (…); and, second, one must discover all possible sources of parametric excitation as well as extraneously, instability-, and movement-induced excitations that might affect these body and fluid oscillators, either individually or in combination, for the given operating conditions." And finally: "Engineers are advised (…) to use the examples [from preceding projects] merely as a means of training themselves in recognizing the basic elements of FIVs (...). Simpler roads or shortcuts to satisfactory engineering solutions do not seem to exist in this complex field of fluid-structure interaction."

2.6 Conclusions from the physical description

Recapping the analytical model paradigms of Sections 2.2-2.4, plus the discussion in Section 2.5, a number of conclusions are drawn with relevance to the computational efforts ahead.

- The added coefficients m_w and c_w central to quantification of dynamic excitations are not readily derived analytically for an oscillating object in a flowing fluid.
- The traditional engineering method of estimating m_w and the steady hydrodynamic forces on a gate, namely by potential flow theory, is too limited to have general computational power. It works only for inviscid, rotation-free flow and thus fails to deal with separated flow and any type of flow where (periodic or non-periodic) fluctuations dominate.
- Self-excitation is typically a non-linear phenomenon. Therefore, all linear models fall short of a full description.
- Applying analytically derived equations as the sole foundation of numerical FIV predictions is troublesome, because of the complex interaction of the fluid-solid process *and* the essential role of empirical factors (e.g. discharge coefficient, lift force coefficient).
- Thus far in literature it has been the rigour of physics-based analysis that is used in the identification of vibration causes and in the search for suitable remedies. But the apparent orderly dinstinctions between different excitation types and between different added coefficients are in practice much less obvious. There can be –and often are– combinations of the mechanisms. Moreover, when more than one d.o.f. comes into play the number of possible physical descriptions explodes and the intangibility tends to make explanations of oscillation origins more subjective.

- Realising that a gate is part of a compound structure with innumerous structural parts, some of which are influencing the flow around the structures, makes matters even worse in terms of predicting whether FIVs will occur.

In conclusion, new methods for analysis and computations are welcomed. Real-life problem solving would benefit in particular from computational techniques that establish or refute connections between dominant eigenmodes and excitation mechanisms.